

Charge radii in the $50 \leq N, Z \leq 82$ region

R. Turcotte and N. de Takacsy

Department of Physics, McGill University, Montreal, Quebec, Canada H3A 2T8

(Received 25 February 1988)

It is shown that the isotopic variation in charge radii for selected nuclei in the $50 \leq N, Z \leq 82$ region can be described in a shell model framework using a semirealistic effective interaction.

I. INTRODUCTION

There exists by now a wealth of data on the variation with neutron number of nuclear charge radii.¹ The simplest interpretation of this data is in terms of the droplet model^{2,3} where the difference between the spherical prediction and the experimental observation defines the effective deformation parameter $\langle \beta^2 \rangle$. Since this is a definition, it is possible that many effects are included in the extracted $\langle \beta^2 \rangle$, in addition to the real deformation effects. It is the purpose of this paper to show that, at least for the nuclei in the $50 \leq N, Z \leq 82$ region, the dominant effect is indeed quadrupole deformation.

II. THE MODEL

The framework for the present calculations is the same in all essentials as that given in Ref. 4. We start from a shell model Hamiltonian:

$$H = \sum_{\alpha} \epsilon_{\alpha} a_{\alpha}^{\dagger} a_{\alpha} + \frac{1}{4} \sum_{\alpha\beta\gamma\delta} V_{\alpha\beta\gamma\delta} a_{\alpha}^{\dagger} a_{\beta}^{\dagger} a_{\gamma} a_{\delta} . \quad (1)$$

The single particle labels are restricted to one major shell consisting of the $1d_{5/2}$, $0g_{7/2}$, $2s_{1/2}$, $1d_{3/2}$, and $0h_{11/2}$ orbitals. The two-body matrix elements are calculated using the nonlocal Tabakin potential⁵ which gives a reasonable fit to the nucleon-nucleon phase shifts and harmonic oscillator wave functions with a fixed size parameter ($\hbar\omega = 8.1$ MeV). They are renormalized by including all the second order ladder graphs, and a very limited set of core polarization graphs. The single particle energies ϵ_{α} are determined by a fit to the one quasiparticle energies in the Sn isotopes, and the $N = 82$ isotones. These calculations are done⁶ using a spherical Bardeen-Cooper-Schrieffer (BCS) code, and the results are listed in Table I. Some two body matrix elements are also modified in order to improve the agreement with these data: all the $T = 1$ matrix elements connecting the $(0h_{11/2})^2$ configuration to itself and to the $(0g_{7/2})^2$ and the $(1d_{5/2})^2$ configurations are multiplied by 1.3 and a small (anti-)pairing force ($G_{\pi} = -0.04$ MeV fm⁻³) is added to the proton-proton interaction. These single particle energies and matrix element modifications differ only in detail from those of Ref. 4 primarily because of the availability of new data. We did not refit the quadrupole effective charges; the earlier calculations had given $e_{\pi} = 1.7$ and $e_{\nu} = 1.1$. These values were obtained by comparing the results of a spherical quasiparticle Tamm-Dancoff ap-

proximation (TDA) calculation to the experimental $B(E2)$ for the semimagic nuclei. The importance of using a semirealistic interaction has been discussed many times before, for example in Refs. 4 and 7.

Since complete shell model calculations are prohibitively lengthy, the structure of the deformed nuclei away from the closed shells is obtained through an axially symmetric deformed Hartree-Fock-BCS calculation: the poor man's shell model. In brief, the intrinsic state is written

$$| \text{intr}(\beta, \gamma) \rangle = \prod_{i,k} (u_{\pi,i,k} - v_{\pi,i,k} a_{\pi,i,k}^{\dagger} \bar{a}_{\pi,i,k}) \times \prod_{i,k} (u_{\nu,i,k} - v_{\nu,i,k} a_{\nu,i,k}^{\dagger} \bar{a}_{\nu,i,k}) | 0 \rangle , \quad (2)$$

$$a_{i,k}^{\dagger} = \sum_{n,l,j} c_{n,l,j,i,k} a_{n,l,j,k}^{\dagger} , \quad (3)$$

where the operator $a_{\pi,i,k}^{\dagger}$ creates a proton in a deformed orbital, k labels the 3 component of angular momentum, and i is an arbitrary sequence label. Neutrons are labeled by ν and the bar indicates a time reversed state. The deformation parameter β is defined below, and γ can be either 0 or $\pi/3$, corresponding to prolate or oblate shapes. The deformed orbitals are, as usual, expanded in a spherical basis, and, in this case, only the one major shell is included.

The Nilsson coefficients and the occupation amplitudes are obtained by minimization

$$\delta \langle \text{intr}(\beta, \gamma) | H + \lambda(Q_{\pi} + Q_{\nu}) | \text{intr}(\beta, \gamma) \rangle = 0 , \quad (4)$$

which leads to the usual Hartree-Fock and BCS equations. The operator Q_{π} and Q_{ν} are the usual quadrupole moment operators for protons and neutrons. The Lagrange multiplier λ determines the deformation pa-

TABLE I. Single particle energies with respect to the ¹⁰⁰Sn core.

	Tabakin		Pairing + quadrupole	
	Proton	Neutron	Proton	Neutron
$1d_{5/2}$	0.459	0.0	0.96	-2.55
$0g_{7/2}$	0.0	0.100	0.0	-2.43
$2s_{1/2}$	2.295	1.972	2.75	-0.33
$1d_{3/2}$	2.568	2.326	2.90	0.0
$0h_{11/2}$	3.190	3.028	3.10	-0.05

rameters β and γ , and makes it possible to vary the deformation of the intrinsic state, though only within limits. The intrinsic state can always be constrained to a spherical, or a prolate, or an oblate shape, but the deformation is limited at the upper end by the restriction of the vector space to one major shell and at the lower end by the value of λ which produces a prolate-oblate shape change rather than a further decrease in the size of the quadrupole moment.

The deformation parameter β is defined to have the usual Bohr-Mottelson meaning. It is extracted from the intrinsic state by taking the ratio of the microscopically calculated quadrupole moment and the liquid drop estimate:

$$\langle \text{intr}(\beta) | e_{\pi} Q_{\pi} + e_{\nu} Q_{\nu} | \text{intr}(\beta) \rangle = \frac{3}{\sqrt{5\pi}} Z e R_0^2 \beta (1 + 0.36\beta). \quad (5)$$

While it is reasonable to describe a well deformed axially symmetric nucleus in terms of a single intrinsic state (calculated with $\lambda=0$), the nuclei in which we are interested have spectra that characterize them as moderately deformed and gamma soft. We therefore use the above formalism to generate a deformed energy surface (and include a Coulomb energy correction for good measure):

$$V(\beta, \gamma) = V_0(\beta) + V_1(\beta) \cos(3\gamma), \quad (6)$$

$$V_0(\beta) = \frac{1}{2} \left[\langle \text{intr}(\beta, 0) | H | \text{intr}(\beta, 0) \rangle + \left\langle \text{intr} \left[\beta, \frac{\pi}{3} \right] | H | \text{intr} \left[\beta, \frac{\pi}{3} \right] \right\rangle \right] - \frac{3}{20\pi} \frac{Z^2 e^2}{R_0} \beta^2, \quad (7)$$

$$V_1(\beta) = \frac{1}{2} \left[\langle \text{intr}(\beta, 0) | H | \text{intr}(\beta, 0) \rangle - \left\langle \text{intr} \left[\beta, \frac{\pi}{3} \right] | H | \text{intr} \left[\beta, \frac{\pi}{3} \right] \right\rangle \right] \quad (8)$$

A simple interpolation formula is used to generate $V_0(\beta)$ and $V_1(\beta)$ on an evenly spaced coordinate grid starting from the very unevenly spaced results of the Hartree-Fock-BCS calculation.

The nuclear wave function is the solution of the Bohr Hamiltonian,^{8,9}

$$[E - T_{\text{vib}} - T_{\text{rot}} - V(\beta, \gamma)] \Psi(\beta, \gamma, \theta_1, \theta_2, \theta_3) = 0, \quad (9)$$

$$T_{\text{rot}} = \frac{J_1^2}{2\mathcal{J}_1} + \frac{J_2^2}{2\mathcal{J}_2} + \frac{J_3^2}{2\mathcal{J}_3}, \quad (10)$$

$$\mathcal{J}_k = 4D\beta^2 \sin^2(\gamma - \frac{2}{3}k\pi), \quad (11)$$

$$T_{\text{vib}} = -\frac{\hbar^2}{2D} \left[\frac{1}{\beta^4} \frac{\partial}{\partial \beta} \beta^4 \frac{\partial}{\partial \beta} + \frac{1}{\beta^2 \sin 3\gamma} \frac{\partial}{\partial \gamma} \sin 3\gamma \frac{\partial}{\partial \gamma} \right]. \quad (12)$$

The ground state ($J=0$) wave function is independent of Euler angles, and can be written

$$\Psi(\beta, \gamma) = \sum_l \left[\frac{2l+1}{2} \right]^{1/2} \Phi_l(\beta) P_l[\cos(3\gamma)]. \quad (13)$$

The series is very rapidly convergent if the prolate-oblate energy difference is modest. For simplicity, the inertial parameter D is taken to be independent of deformation and is determined for each nucleus by fitting the experimental 0^+ to 2^+ energy difference in the gamma soft ($V_1=0$) limit of the Bohr model (where the solutions are also simple). This is the one parameter that is adjusted separately for each nucleus.

The nuclear deformation, including shape oscillations, is then

$$\langle \beta^2 \rangle = \sum_l \int \Phi_l^2 \beta^6 d\beta. \quad (14)$$

The model is now completely defined, but, by its nature, it cannot directly predict nuclear sizes. In fact, at a first level, the size information is an input into the calculation of the two-body matrix elements which are then held fixed. However, the model is essentially parameter free, and it does predict the general structure and specifically the ground state deformation of any even-even nucleus between the magic numbers 50 and 82. It therefore complements the droplet model² and the two can be combined to predict the variation of nuclear sizes with neutron number. The model is similar to the one used by Myers and Rozmej¹⁰ to study the Rb isotopes.

III. RESULTS

Since the isotope shift data^{1,11} on the Ba isotopes is both accurate and extensive, we start by concentrating on these. The results of the calculation are shown in Table II which lists the location of the energy minima along the prolate and oblate axes, the deduced value of the inertial parameter D , and the computed rms deformation. The experimental deformation parameters are extracted in the usual way:

$$\delta \langle r^2 \rangle_{\text{expt}}^{82, N} = \delta \langle r^2 \rangle_{\text{droplet}}^{82, N} + \frac{5}{4\pi} \langle r^2 \rangle_{\text{droplet}}^{(N)} \delta \langle \beta^2 \rangle_{\text{expt}}^{82, N}. \quad (15)$$

The superscripts indicate that the changes are with respect to the reference nucleus with 82 neutrons and the droplet model quantities are calculated in the spherical limit. The data are compared to the calculations in Fig. 1 and Table II.

For completeness, we show in Fig. 2 the calculated energy functions $V_0(\beta)$ and $V_1(\beta)$ for the typical case of ¹³⁰Ba and in Fig. 3 the spectrum of energy levels for the same nucleus calculated in the gamma-soft limit, along with the experimental data.¹² It is not our purpose here to do detailed spectroscopic calculations for these nuclei, but only to argue that the model gives a good description of the structure of the Ba nuclei. It is nevertheless worth noting that V_1 is in fact small, and that its proper inclusion in the calculation would produce small deviations from the classical gamma-soft spectrum.¹³ Actually, we expect that a more careful treatment of the proton-neutron collective dynamics would be profitable when studying the relative spacing of the levels in the $2_1^+, 4_1^+$

TABLE II. Deformations in the Ba isotopes using a semirealistic interaction derived from the Tabakin potential. The columns labeled ΔE give the calculated energy differences between the spherical and the deformed solutions. The experimental deformation parameters are normalized to the theoretical value at $N = 82$.

A	D (MeV^{-1})	Prolate		Oblate		$\sqrt{\langle \beta^2 \rangle}$	
		β_{\min}	ΔE_{\min}	β_{\min}	ΔE_{\min}	Calc.	Expt.
138	220	0.0	0.0	0.0	0.0	0.089	0.089
136	215	0.11	-0.43	-0.10	-0.31	0.117	0.123
134	185	0.18	-1.91	-0.16	-1.34	0.146	0.160
132	160	0.21	-3.79	-0.20	-2.74	0.176	0.190
130	150	0.23	-5.69	-0.24	-4.42	0.200	0.214
128	140	0.25	-7.26	-0.27	-6.26	0.226	0.235
126	125	0.27	-8.31	-0.30	-7.94	0.255	0.253
124	140	0.28	-8.53	-0.32	-8.77	0.258	0.269
122	155	0.28	-8.57	-0.31	-8.89	0.260	0.286
120	170	0.28	-8.46	-0.31	-8.75	0.269	

doublet and the $3_1^+, 4_2^+, 6_1^+$ triplet. Specifically, the neutrons and the protons should perhaps be described by different deformation variables. Of course, the $J=0^+$ ground state wave functions which determine $\langle \beta^2 \rangle$ are obtained using the full Bohr Hamiltonian.

The same comparison of theory and experiment can be done for the Xe, Nd, and Sm (Refs. 14 and 15) isotope sequences, and with much the same results. This is shown in Fig. 4 where the calculated and experimental deformations of the $N=76$ isotones are plotted as a function of atomic number.

It is clear that there is good agreement between theory and experiment in all these cases. The predicted deformations are systematically somewhat too small (by $\sim 10\%$), and there is a good reason for this. The scale of the theoretical β depends on the values chosen for the shell model effective charges, and the assumption that they are independent of deformation. However, one expects that the importance of across shell excitations

should increase with deformation, and our model does not take this into account. In fact, it is very satisfactory to observe that this effect is so small. To put it another way, the restriction of the vector space to one major shell limits the range of quadrupole moments accessible to a system with fixed Z and N with the result that there is a very strong and rapid rise in the Bohr potential $V_0(\beta)$ for values of β past the minimum, and a consequent and unphysical truncation of the high β tail of the wave function.

There is also a small but systematic difference in slope between the data and the calculation for the Ba isotopes near $N=66$. The theoretical deformations tend to saturate in this region, and then decrease back to near sphericity as $N \rightarrow 50$. The data on the contrary show a continued and almost linear increase in $\langle \beta^2 \rangle$ right through the lightest measured isotope. The same discrepancy also shows up in the $E(4^+)/E(2^+)$ ratios in the light Ba (though not in the Xe) isotopes.¹⁶

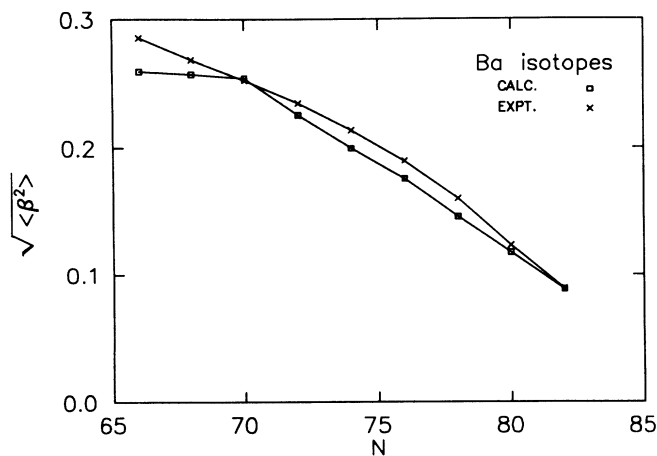


FIG. 1. Calculated and experimental deformation of the Ba isotopes. The calculations are based on the Tabakin interaction. The experimental points are taken from the isotope shift data and are normalized to the theory at $N = 82$.

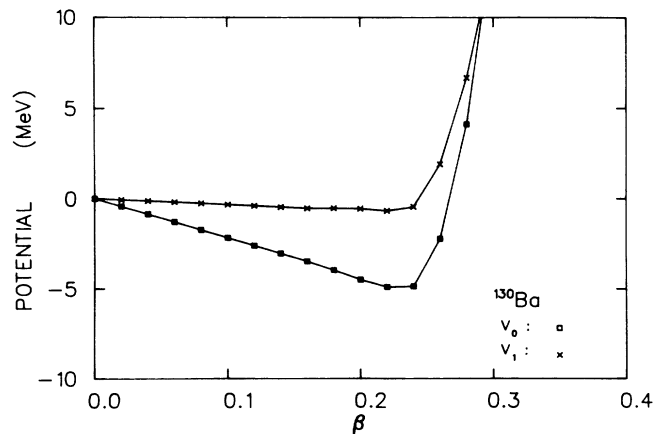


FIG. 2. The potential energy function of the Bohr Hamiltonian for ^{130}Ba derived using the Tabakin interaction.

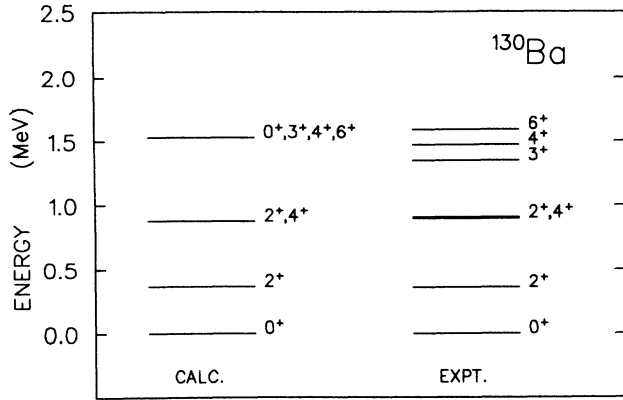


FIG. 3. The energy levels of ^{130}Ba calculated in the gamma-limit of the Bohr model using the Tabakin interaction.

We therefore conclude that, at least in this region of the periodic table ($50 \leq N, Z \leq 82$), nuclear deformations can be predicted in an essentially parameter-free way within the general framework of the shell model, and nuclear deformation can explain the major part of the differences between the measured charge radii and the predictions of the spherical droplet model.

Another way to show this is to use the predicted deformation parameters as input to the droplet model.^{2,3} We can then compare the experimental radius differences to the predictions of the deformed droplet model, and extract a residual difference which is most conveniently parametrized in terms of a "residual deformation" parameter $\langle \beta^2 \rangle_{\text{res}}$ which then contains all the effects *other* than quadrupole deformation,

$$\delta \langle r^2 \rangle_{\text{expt}}^{N',N} = \delta \langle r^2 \rangle_{\text{droplet}}^{N',N}(\beta) + \frac{5}{4\pi} \langle r^2 \rangle_{\text{droplet}}^{(N)}(\beta) \delta \langle \beta^2 \rangle_{\text{res}}^{N',N}. \quad (16)$$

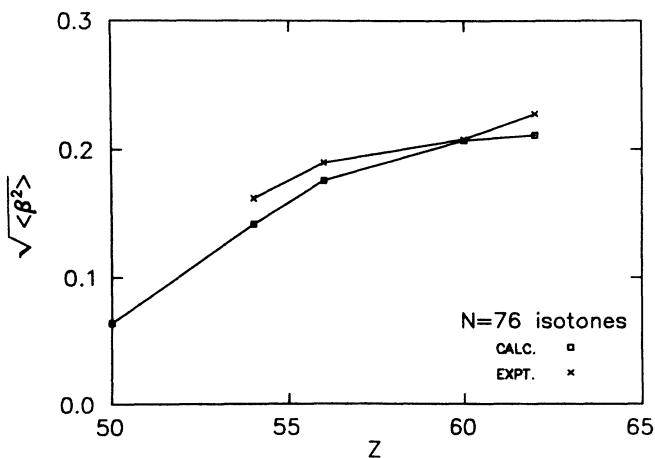


FIG. 4. The calculated and experimental deformation of the $N = 76$ isotones. The calculations are based on the Tabakin interaction. The experimental points are taken from the isotope shift data and are normalized to the theory for each isotope at $N = 82$.

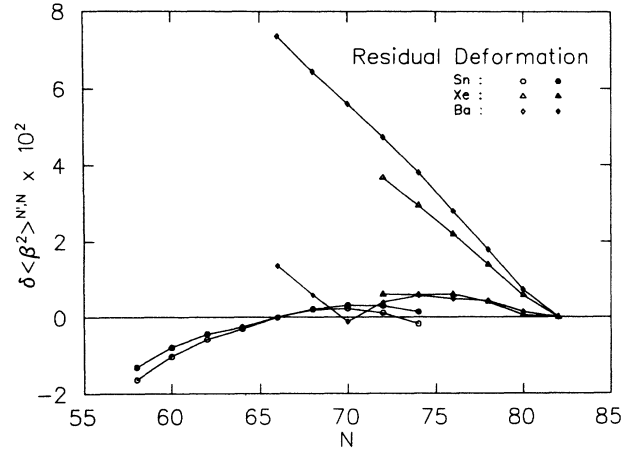


FIG. 5. The differences between the experimental and droplet model mean square radii for the Ba, Xe, and Sn isotopes, expressed as effective deformations. The open symbols refer to the spherical droplet model and the solid symbols to the deformed droplet model with the magnitude of the deformation taken from theory. $N' = 82$ for Ba and Xe, and $N' = 66$ for Sn.

We have done this for the Ba, Xe, and Sn (Refs. 17 and 18) isotopes with the results shown in Fig. 5. The open and solid symbols show the data compared to the spherical and the deformed droplet models, respectively, where the deformation is predicted by the calculations. It is clear that the residual effects are small once the deformation is properly included.

The case of the Sn isotopes warrants further comment. As expected for semimagic nuclei, the calculated deformations are small for all the isotopes, and reach a maximum at ^{116}Sn with $\sqrt{\langle \beta^2 \rangle} = 0.096$, which is about 10% smaller than the experimental value $\sqrt{\langle \beta^2 \rangle} = 0.103$ from Coulomb excitation.¹⁹ The isotope shift data are in good agreement with these small values of the dynamic deformation except for the lightest isotopes where a regular curvature in the data becomes manifest. From our results we have to conclude that this curvature is not due to quadrupole deformation of the valence nucleons, and cite the observed systematics^{19,20} in the energy and the $B(E2)$ of the 2_1^+ state in support of this. More subtle explanations have been proposed,²¹ and it is also reasonable to expect that the intruder band^{22,23} that occurs near $N = 66$ should have an effect.

IV. A SCHEMATIC HAMILTONIAN

Although the use of a semirealistic Hamiltonian has important advantages,^{4,7} the results obtained above do not depend qualitatively on this choice. To prove this, we have repeated the calculations for the Ba isotopes using a standard pairing plus quadrupole interaction. The single particle energies are given in Table I, and the strength of the pairing force is $G_\pi = G_\nu = 0.25$ MeV. The quadrupole potential is

$$V_{q-q} = -\kappa \frac{5}{32\pi} (Q_\pi + Q_\nu)(Q_\pi + Q_\nu), \quad (17)$$

TABLE III. Deformation in the Ba isotopes using a pairing plus quadrupole interaction. The columns labeled ΔE give the calculated energy differences between the spherical and the deformed solutions. The experimental deformation parameters are normalized to the theoretical value at $N = 82$.

A	D (MeV^{-1})	Prolate		Oblate		$\sqrt{\langle \beta^2 \rangle}$	
		β_{\min}	ΔE_{\min}	β_{\min}	ΔE_{\min}	Calc.	Expt.
138	240	0.0	0.0	0.0	0.0	0.087	0.087
136	225	0.0	0.0	0.0	0.0	0.118	0.122
134	200	0.16	-1.06	-0.12	-0.29	0.142	0.159
132	175	0.20	-2.83	-0.17	-1.29	0.171	0.189
130	155	0.23	-4.55	-0.21	-2.60	0.203	0.214
128	145	0.25	-5.80	-0.26	-3.90	0.232	0.234
126	130	0.26	-6.81	-0.29	-5.46	0.257	0.252
124	135	0.27	-7.52	-0.30	-6.23	0.266	0.269
122	160	0.28	-7.64	-0.29	-5.45	0.262	0.285

where $\kappa = 0.00444 \text{ MeV fm}^{-4}$. These form a reasonable parameter set, and there is no need for a particularly careful choice for the present purposes. The single particle energies are close to the data for ^{131}Sn and ^{133}Sb ,^{24,25} and also to the energies used with the more realistic Hamiltonian when the N - and Z -dependent monopole mean field of the latter is taken into account. The strength of the pairing force is roughly determined by the observed pairing gap in the $N = 82$ and the $Z = 50$ nuclei. Finally, the strength of the quadrupole interaction is chosen to roughly reproduce the calculated deformation of ^{130}Ba with the more realistic Hamiltonian.

The results of the calculation are given in Table III. They are essentially the same as those obtained using the Tabakin potential, except that deformation sets in a little more slowly near $N = 82$, and the deformed energy minimum is more shallow. We expect the difference to be more significant if the space spans more than one major shell.

V. CONCLUSIONS

It was shown that the structure, and, more specifically, the deformation of nuclei in the $50 \leq N, Z \leq 82$ can be predicted using a semirealistic interaction derived from the Tabakin potential. The calculated deformations can

be used as input to the droplet model with a standard parametrization in order to predict the variation with neutron number of nuclear charge radii. The results are in generally good agreement with the data extracted from isotope shift measurements for long isotope chains.

The calculation uses a Hartree-Fock-BCS formalism, but the basic framework is the shell model with its strengths and its limitations. The vector space is restricted to a single major shell, the harmonic oscillator size parameter is fixed, and the across shell admixtures are incorporated through constant effective charges. In these respects the model is different from the more ambitious Hartree-Fock calculations that span a large vector space.^{10,26,27,28} Its predictions are also quantitatively different, especially with respect to the onset of deformation near a spherical magic number, and the energy gain that accrues with deformation.

ACKNOWLEDGMENTS

This work was supported in part by the Natural Sciences and Engineering Research Council of Canada and the Fonds FCAR pour l'Aide et le Soutien à la Recherche du Gouvernement du Québec. We thank F. Buchinger for many useful discussions on the subject of isotope shift measurements and their interpretation.

¹P. Aufmuth, K. Heilig, and A. Steudel (unpublished).

²W. D. Myers and K.-H. Schmidt, Nucl. Phys. A **410**, 61 (1983).

³W. D. Myers, *Droplet Model of Atomic Nuclei* (Plenum, New York, 1977).

⁴N. de Takacsy and S. Das Gupta, Phys. Rev. C **13**, 399 (1976).

⁵F. Tabakin, Ann. Phys. (N.Y.) **30**, 51 (1964).

⁶R. Turcotte, Ph.D. thesis, McGill University, 1988.

⁷R. A. Sorensen, Nucl. Phys. A **420**, 221 (1984).

⁸J. P. Davidson, *Collective Models of the Nucleus* (Academic, New York, 1968).

⁹A. Bohr and B. R. Mottelson, *Nuclear Structure* (Benjamin, New York, 1975), Vol. 2.

¹⁰W. D. Myers and P. Rozmej, Nucl. Phys. A **470**, 107 (1987).

¹¹A. C. Mueller, F. Buchinger, W. Klempt, E. W. Otten, R.

Neugart, C. Ekstrom, and J. Heinemeier, Nucl. Phys. A **403**, 234 (1983).

¹²Sun Xiangfu, D. Bazzacco, W. Gast, A. Gelberg, U. Kaup, A. Dewalt, K. O. Zell, and P. von Brentano, Phys. Rev. C **28**, 1167 (1983).

¹³J. Dobaczewsky, S. G. Rohozinski, and J. Srebny, Z. Phys. A **282**, 203 (1977).

¹⁴H. Gerhardt, F. Jeschonnek, W. Makat, E. Mathias, H. Rinneberg, F. Schneider, A. Timmermann, R. Wenz, and P. J. West, Hyperfine Inter. **9**, 175 (1981).

¹⁵G. D. Alkhozov, A. E. Barzakh, V. N. Buyanov, V. P. Derisov, V. S. Ivanov, V. S. Letokhov, V. I. Mishkin, S. K. Sekatsky, V. N. Fedoseev, and I. Ya. Chubukov (unpublished).

¹⁶G. Puddu, O. Scholten, and T. Otsuka, Nucl. Phys. A **348**, 109

- (1980).
- ¹⁷J. Eberz, U. Dinger, G. Huber, H. Lochmann, R. Menges, G. Ulm, R. Kirchner, O. Klepper, T. U. Kuhl, and D. Marx, *Z. Phys. A* **326**, 121 (1987).
- ¹⁸M. Anselment, K. Bekk, A. Hanser, H. Hoeffgen, G. Meisel, S. Goring, H. Rebel, and G. Schatz, *Phys. Rev. C* **34**, 1052 (1986).
- ¹⁹R. Graetzer, S. M. Cohick, and J. X. Saladin, *Phys. Rev. C* **12**, 1462 (1975).
- ²⁰C. M. Lederer and V. S. Shirley, *Table of Isotopes* (Wiley, New York, 1977).
- ²¹D. Berdichevsky, R. Fleming, and D. W. L. Sprung, *Bull. Am. Phys. Soc.* **32**, 1562 (1987).
- ²²J. Kantele, R. Julin, M. Luontama, A. Passoja, T. Poikolainen, A. Bäcklin, and N.-G. Jonsson, *Z. Phys. A* **289**, 157 (1979).
- ²³A. Aprahamian, D. S. Brenner, R. F. Casten, R. L. Gill, A. Piotrowski, and K. Heyde, *Phys. Lett.* **140B**, 22 (1984).
- ²⁴B. Fogelberg and J. Blomqvist, *Phys. Lett.* **137B**, 20 (1984).
- ²⁵J. Blomqvist, A. Kerek, and B. Fogelberg, *Z. Phys. A* **314**, 199 (1983).
- ²⁶G. Audi, A. Coc, M. Epherre-Rey-Campagnolle, G. Le Scornet, C. Thibault, and F. Touchard, *Nucl. Phys. A* **449**, 491 (1986).
- ²⁷X. Campi and M. Epherre, *Phys. Rev. C* **22**, 2603 (1980).
- ²⁸N. Redon, J. Meyer, M. Meyer, P. Quentin, M. S. Weiss, P. Bonche, H. Flocard, and P. H. Heenen, *Phys. Lett. B* **181**, 223 (1986).